Apply Grey Relation Analysis to Identify and Characterize Inter-well Interference Based on the Tracer Monitoring in the Mahu Sag

Wenfeng Liu
Baikouquan oil production plant
Xinjiang Oilfield Company
Xinjiang, China
liuwenfeng@petrochina.com.cn

Chuanyi Tang
Baikouquan oil production plant
Xinjiang Oilfield Company
Xinjiang, China
tchuanyi@petrochina.com.cn

Xiaolun Yan
China University of Petroleum (Beijing)
College of Petroleum Engineering
Beijing, China
yan921259331@163.com

Huazhi Xin
Baikouquan oil production plant dept.
Xinjiang Oilfield Company
Xinjiang, China
xhz-xj@petrochina.com.cn

Xin Liu
Baikouquan oil production plant
Xinjiang Oilfield Company
Xinjiang, China
syliuxin@petrochina.com.cn

Xubin Zhao
Baikouquan oil production plant
Xinjiang Oilfield Company
Xinjiang, China
zxubin@petrochina.com.cn

Abstract—For the unconventional reservoirs, advances in drilling and fracturing technologies prompt operators to tend to the designs of large-scale, staged fracturing with multi-cluster in one stage. However, with the well spacing getting closer, it must be noted that the risk of inter-well interference increases since the hydraulic fractures can interfere, even hydraulically communicate. In the past few years, inter-well interference became more prominent and thus received significant attention in the development of unconventional reservoirs. The interferences in fracturing to adjacent wells have negative effects as: (1) abnormal changes in wellhead pressure, daily gas production and daily water production of adjacent wells; (2) water flood out, mud backflow or sand production, etc. In some extreme cases, production wells may never fully recover or stop production permanently.

In this paper, we study inter-well and interlayer interferences as well as casing deformation in Mahu 131 block using fluid tracer monitoring, Grey Relation Analysis (GRA), and micro-seismic monitoring and analysis. Firstly, tracer monitoring results are analyzed after fracturing. Next, the Grey Relation Analysis (GRA) is applied to identify the connectivity between wells as well as characteristics of the interference. In addition, the micro-seismic monitoring and analysis is used to explain the mechanism of interlayer interference and casing deformation risk caused by the multi-stage fracturing.

The results indicate that the type of interference (same layer, inter-layer) and the well section interfered can be directly determined through fracturing fluid tracer monitoring. Grey Relation Analysis (GRA) is an effective way to clarify the connectivity of different fractured intervals for complicated flow. Abnormal micro-seismic signals and sever interference events are found to occur more likely in fracture warms and faults where weak planes are easier to be dislocated and cracked. This coupling effect will increase the risk of casing deformation in horizontal wells.

Keywords—interference, GRA, tracer monitoring, fracturing, horizontal well

I. INTRODUCTION

The Triassic Baikouquan formation of Mahu 131 block is structurally located in the north slope area of Mahu sag, the central depression of Junggar basin (Fig 1). According to lithology and electrical characteristics (Fig 2), this formation is divided into three sections as T_1b_1, T_1b_2 and T_1b_3 from bottom to top. Among them, the section of T_1b_2 is composed of two sand beds including $T_1b_2^1$ and $T_1b_2^2$ from top to bottom, and the oil reservoir is mainly distributed in T_1b_3 and $T_1b_2^2$.

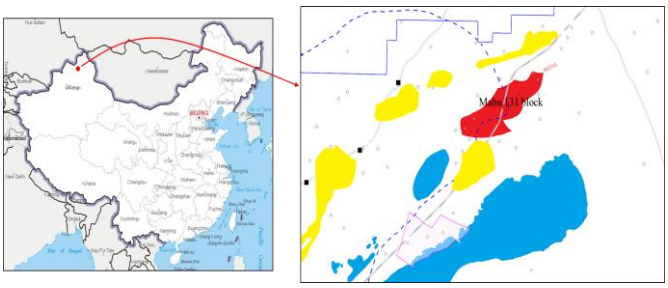

Fig. 1. The Triassic Baikouquan formation of Mahu 131 block.

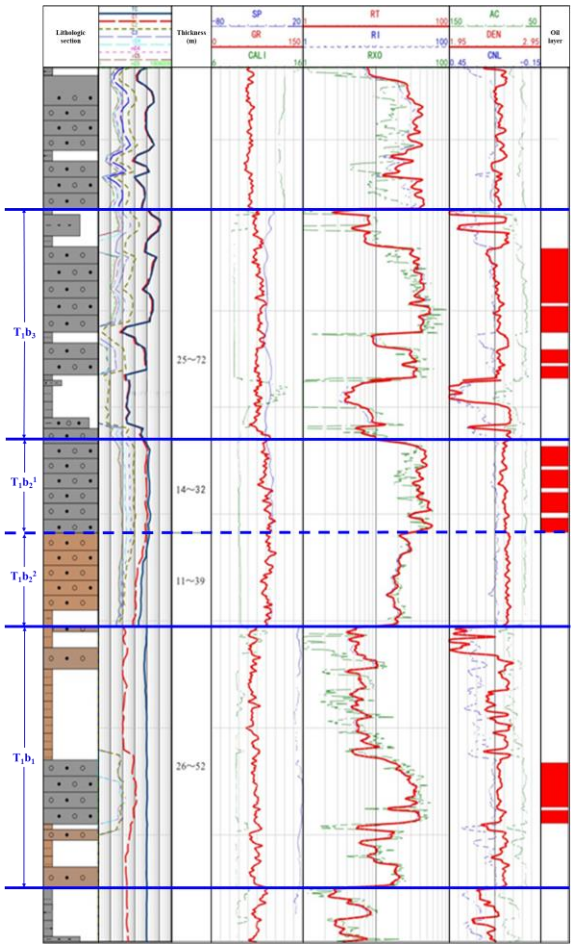

Fig. 2. Type log for the Triassic Baikouquan formation of Mahu 131 block

As shown in Fig.3, the reservoir lithology is mainly gray sandy conglomerate, pebbly coarse sandstone, sandy conglomerate, medium coarse conglomerate and calcareous sandy conglomerate, etc. The statistical results of rock thin sections from 10 wells contains: 57.1% gravel, 36.9% sandy component, 4.3% miscellaneous base, and 1.3% cement (Fig.4).

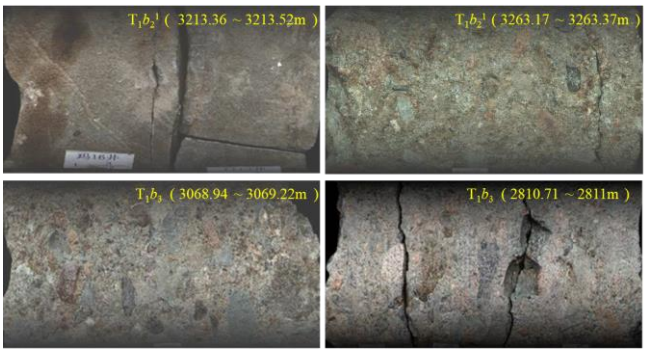

Fig. 3. Core pictures for the Triassic Baikouquan formation of Mahu 131 block

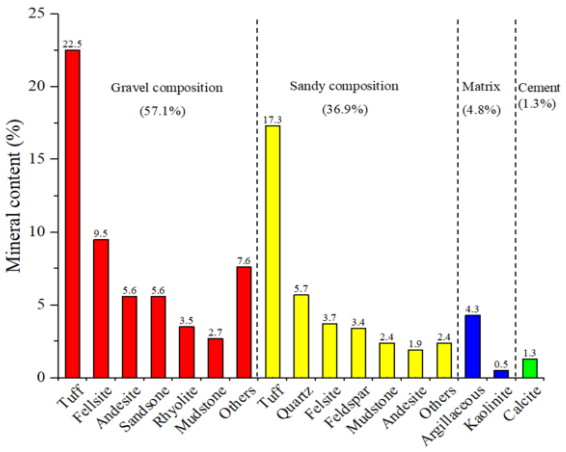

Fig. 4. Mineral composition statistics

The average porosity and permeability of the T_1b_3 formation are 8.26% (5% - 14.3%) and 0.89md (0.02mD ~ 17.2mD), which are 7.63% (5% - 13.9%) and 1.33mD (0.02mD - 9.4mD) in the $T_1b_2^1$ formation. According to the classification of conglomerate reservoirs, these belong to the ultra-low porosity and low-permeability type IV reservoirs which must be effectively fracture stimulated for commercial production. On the base of earlier testing in Mahu, horizontal wells with long laterals were drilled and fractured by using multiple stages with large amounts of slick-water and sand in October 2016, and severe inter-well interference events were followed. Up to now, there are 92 horizontal oil wells have been put into production and 54.3% of them interfered with adjacent wells. The total number of fracturing stimulated stages is 1870 and 140 of them were interfered with fracturing, accounting for 7.5%.

This was demonstrated in several studies that the fluid flow during the period post-stimulation "flowback" described the connectivity between wells as a whole [1] [2] [3]. A series of assessment methods and surveillance techniques have been developed to evaluate the complicated relevance of inter-well interference [4] [5] [6]. Nevertheless, any single method or surveillance technique has inherent limitations and biases in varying degrees. To gain a comprehensive understanding on the complexity of inter-well interference, multiple means must be combined effectively through various ways to enhance the reliability of analysis results [7].

II. PROJECTIONS

Pad Layout Setting

Three multi-well horizontal pads consisting of two formations completed in the Mahu 131 demonstration district: T_1b_3 and $T_1b_2^1$. The upper formation (T_1b_3) comprises seven wells (X46-X52), while five wells (X41-X45) were drilled in the lower formation ($T_1b_2^1$). The layout setting and vertical cross-section of these three pads are illustrated in Fig.5. The vertical spacing for T_1b_3 $T_1b_2^1$ wells is approximately 35-40m. The horizontal distance between the wells varies by formation while spacing within each formation is held relatively consistent.

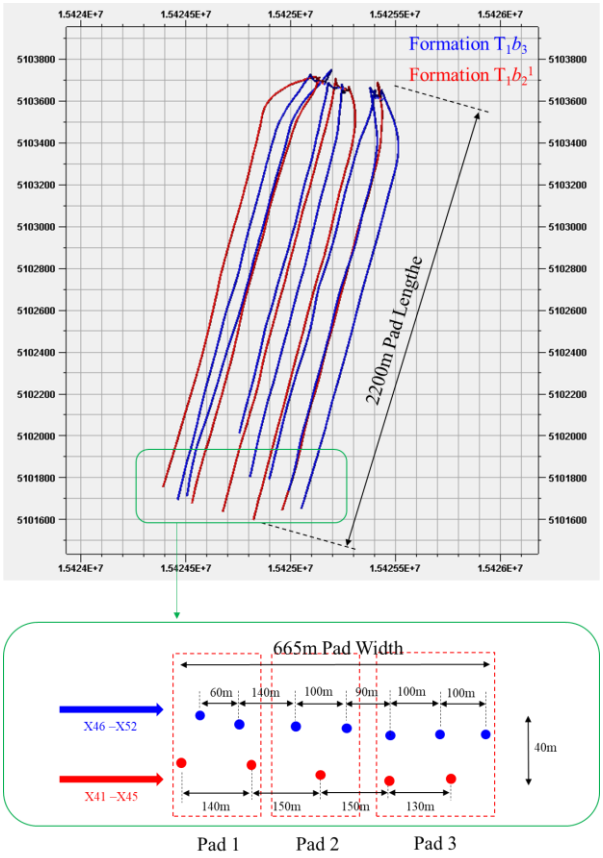

Fig. 5. Pad layout of the target well pads and vertical cross-section of the pads

Completion and Stimulation Practices

The summary of well and completion information is listed in Table I. Typical lateral lengths are 1489 to 1802m and each well has 24 to 33 frac stages. Approximately 500 to 1200 m³of slick water and 50 to 100 m³of sand are pumped per stage at rates up to 12 m³per minute, while viscous gel slugs are used for complex fracture network. These pads are multi fractured applying frac 'wave' concept.

TABLE I. SUMMARY OF THE WELL AND COMPLETION INFORMATION

Well	Formation	Pad	Total Stages	Injected Fluid Volume (m^3)	Proppant Volume (m^3)
X41	$T_1b_2^1$	1	26	34521.4	2125
X42	$T_1b_2^1$	1	24	48789.6	3245
X43	$T_1b_2^1$	2	29	54121.5	3380
X44	$T_1b_2^1$	3	29	51134.3	3250
X45	$T_1b_2^1$	3	27	36452.0	2190
X46	T_1b_3	1	33	24274.5	1900
X47	T_1b_3	1	29	23051.9	1890
X48	T_1b_3	2	26	21622.0	1692
X49	T_1b_3	2	27	21111.4	1670
X50	T_1b_3	3	27	28764.7	2510
X51	T_1b_3	3	26	29220.5	2700
X52	T_1b_3	3	28	20663.7	1678

Tracers Surveillance

Wells interact as a system in formations, and the transfer of injected frac fluid reveals the connections between wells. Compared to other surveillance technologies, the frac fluid tracer data is more reliable. The tracer surveillance carried out in the Mahu 131 demonstration district date from August 30, 2019. Tracers matching with each stage are pumped with fracturing fluid while the well X43 and X48 fracturing stimulated. The general surveillance results are illustrated in Table II.

TABLE II. GENERAL SURVEILLANCE RESULTS

Fracturing well	Adjacent well	Traces contained in water sample
X43	X41	Tracer-02/10/13/14/19
	X42	Tracer -02/10/13/14/19/25
	X44	Tracer -02/10/13/14/19
	X45	Tracer -02/10/13/14/19
	X46	Tracer -02/10/13/14/19
	X47	Tracer -02/10/13/14/19/25
	X49	Tracer -02/10/13/14/19/25
	X50	Tracer -02/04/10/13/14/19
	X51	Tracer -02/10/13/14/19
	X52	Tracer -02/10/13/14
X48	X41	Tracer -01/02/03/04/14/15/17/23
	X42	Tracer -01/02/03/04/11/14/15/17/18/23
	X44	Tracer -01/02/03/04/11/14/17/18/23
	X45	Tracer -01/02/03/04/08/14/15/17/18/23
	X46	Tracer -01/02/03/04/08/11/14/15/17/23
	X47	Tracer -01/02/03/04/08/11/14/15/17/23
	X49	Tracer -01/02/03/04/08/11/14/15/17/18/23
	X50	Tracer -01/02/03/04/08/11/14/17/23
	X51	Tracer -01/02/03/04/08/11/14/15/17/18/23
	X52	Tracer -01/02/03/04/08/14/15/17/18/23

III. METHDOLOGY

Grey Relation Analysis Method

Deng developed the Grey relation analysis (GRA) method originally [8], and has been widely applied in various fields. The grey system theory puts forward the concept of grey relation degree analysis for each subsystem, with the intention to seek the numerical relationship between each subsystem (or factor) in the system through certain methods [9]. Therefore, grey correlation analysis provides a quantitative measure for the development and change of a system, which is very suitable for dynamic process analysis. In the following, we introduce the main procedure of GRA.

Step 1. Collect analysis data and determine the analysis index system according to analysis purposes.

Data sequence is set as the following matrix:

$$\left(X_1^{'}, X_2^{'}, \ldots, X_n^{'}\right) = \begin{pmatrix} x_1^{'}(1) & x_2^{'}(1) & \cdots & x_n^{'}(1) \\ x_1^{'}(2) & x_2^{'}(2) & \cdots & x_n^{'}(2) \\ \vdots & \vdots & \vdots & \vdots \\ x_1^{'}(m) & x_2^{'}(m) & \cdots & x_n^{'}(m) \end{pmatrix} \quad (1)$$

$$X_i^{'} = (x_i^{'}(1), x_i^{'}(2), \cdots, x_i^{'}(m))^T,\ i = 1, 2, \cdots, n \quad (2)$$

Where m is the number of indicators.

Step 2. Identify reference data columns.

$$X_0^{'} = (x_0^{'}(1), x_0^{'}(2), \cdots, x_0^{'}(m)) \quad (3)$$

Step 3. Normalization processing.

Normalize or initialize the original data:

$$x_i(k) = \frac{x_i^{'}(k)}{\frac{1}{m}\sum_{k=1}^{m} x_i^{'}(k)} \quad i = 0, 1, \cdots, n\ ,k = 1, 2, \cdots, m \quad (4)$$

The normalized data sequence is formed into the following matrix:

$$(X_0, X_1, \cdots, X_n) = \begin{pmatrix} x_0(1) & x_1(1) & \cdots & x_n(1) \\ x_0(2) & x_1(2) & \cdots & x_n(2) \\ \vdots & \vdots & \vdots & \vdots \\ x_0(3) & x_1(m) & \cdots & x_n(m) \end{pmatrix} \quad (5)$$

Step 4. Calculation of correlation coefficient.

$$\zeta_i(k) = \frac{\min\limits_i \min\limits_k |x_0(k) - x_i(k)| + \rho . \max\limits_i \max\limits_k |x_0(k) - x_i(k)|}{|x_0(k) - x_i(k)| + \rho . \max\limits_i \max\limits_k |x_0(k) - x_i(k)|} \quad (6)$$

Where $\zeta_i(k)$ is the correlation coefficient of the sequence X_0 and X_1 at time k, $|x_0(k) - x_i(k)|$ is the absolute difference between X_0 and X_1 at time k, $\min\limits_{i=1}^{n} \min\limits_{k=1}^{m} |x_0(k) - x_0(k)|$ is the minimum absolute difference, $\max\limits_{i=1}^{n} \max\limits_{k=1}^{m} |x_0(k) - x_0(k)|$ is the maximum absolute difference.

ρ is the resolution coefficient, $0 < \rho < 1$. If ρ is smaller, the difference between correlation coefficients is larger, and the discrimination ability is stronger. Generally, ρ is 0.5.

Step 5. Calculation of correlation degree.

The correlation degree between the reference sequence and the comparison sequence is the mean value of the correlation coefficient at each time point:

$$r_{0i} = \frac{1}{m}\sum_{k=1}^{m} \zeta_i(k) \quad (7)$$

The larger r_{0i} is, the more similar the characteristics of the comparison data and the reference data are.

Variation Trend of Data Series

From the perspective of grey theory, if the two factors change with a consistent trend in the process of system development that the degree of synchronous change is high, it means that the degree of correlation between them is high; otherwise, it is low. The reservoir dynamic system after the simulation of multi-stages fracturing is very complex and undefined which can be treated as a grey system. The change of tracer concentration in the fracturing wells will cause the change of tracer concentration in the adjacent wells. To a certain extent, the similarity between them reflects the gravity of interference.

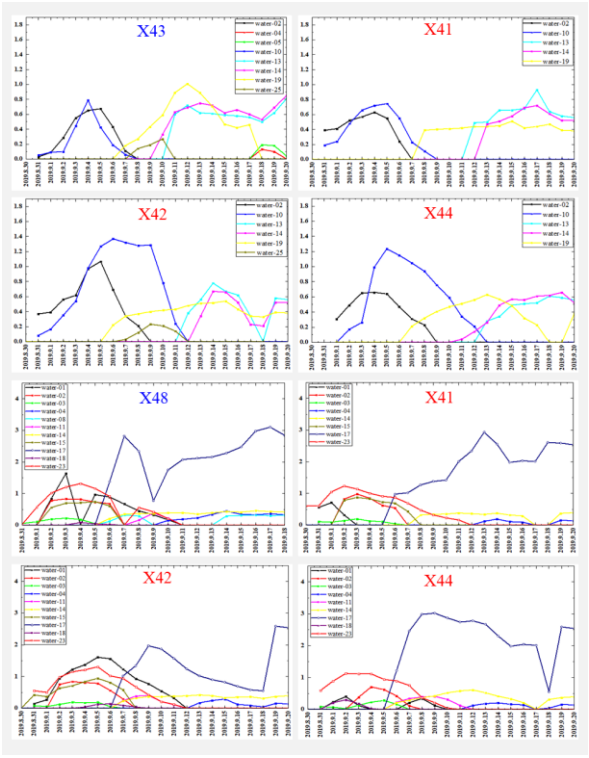

Fig. 6. The overall trend of tracer concentration

In the flowback phase, the general trend of various tracer concentrations changing between fracturing wells and some of adjacent wells is shown in Fig.7. And we can draw some conclusions from this comparison:

- There is a strong correlation between fracturing wells(X43, X48) and adjacent wells about the changes of tracers concentration.
- With the backflow of fracturing fluid, the time change nodes of tracers in adjacent wells are basically the same as these of fracturing wells, and there is no obvious lag.

Interwell Interference Correlation Assesment

The data series of various tracer concentration in fracturing wells reveal the behavior characteristics of the reservoir dynamic system, while these in adjacent wells are the factors affecting the system behavior. Taking two of them as reference sequence and comparison sequence respectively, and the GRA is used to calculate the correlation degree between them, which provides a quantitative measurement for the interference between fracturing wells and adjacent wells. The results are illustrated as Fig.8

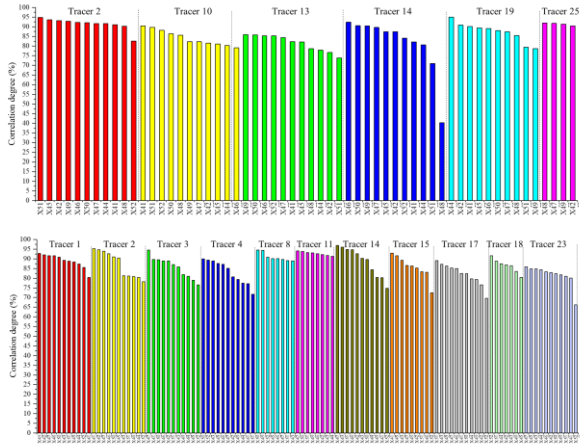

Fig. 7. The interference correlation of wells in different wells

IV. DISCUSSION

Correlations of Fractured Intervals

Base on the results GRA, the summary of interlayer interference events is listed in Table III and the sketch map of them is shown in Fig.9. The connectivity of fractured intervals can be determined by the correlations of fractured intervals:

- A complex fracture network has been formed in the formation of $T_1b_2^1$ .The hydraulic fracture growth vertically, breaking through the mudstone barrier between the formations of T_1b_3 and $T_1b_2^1$, and communicating with the complex fracture network formed between wells in the formation. of $T_1b_2^1$;
- Considering the operation sequence of fracturing pads. Then, the hydraulic fracture growth vertically, breaking through the mudstone barrier between the formations of T_1b_3 and $T_1b_2^1$, communicates with the previously formed fracture network.
- According to the average of correlation degree and the total connected stages, fracturing in the formation T1b3 make greater interference than $T_1b_2^1$. Furthermore, the fracturing sequence of the pads is Pad 3, Pad 1, and Pad 3. It can be concluded that the complex fracture network system formed by the last fracturing of Pad 2, which connects the fractures of the adjacent wells on the left and right and characterized by the fracturing interference between the same layers.

TABLE III. SUMMARY OF INTERLAYER INTERFERENCE EVENTS

Fracturing well (Formation)	Interfered well (Formation)	Connected stages of fracturing well	Average of correlation degree
X43 (T_1b_3)	X46($T_1b_2^1$)	2/10/13/14/19	87.76%
	X47($T_1b_2^1$)	2/10/13/14/19/25	87.94%
	X43($T_1b_2^1$)	2/10/13/14/19/25	78.71%
	X48($T_1b_2^1$)	2/10/13/14/19/25	86.99%
	X49($T_1b_2^1$)	2/4/10/13/14/19	73.90%
	X50($T_1b_2^1$)	2/10/13/14/19	81.84%
	X51($T_1b_2^1$)	2/10/13/14	85.12%
	X52($T_1b_2^1$)	2/10/13/14/19	81.64%
X48	X41(T_1b_3)	1/2/3/4/14/15/17/23	74.67%
($T_1b_2^1$)	X42(T_1b_3)	1/2/3/4/8/14/15/17/18/23	87.49%
	X43(T_1b_3)	1/2/3/4/8/11/14/15/17/18/23	88.17%
	X44(T_1b_3)	1/2/3/4/11/14/17/18/23	84.50%
	X45(T_1b_3)	1/2/3/4/8/14/15/17/18/23	86.63%
	X47(T_1b_3)	1/2/3/4/8/11/14/15/17/23	90.39%
	X49(T_1b_3)	1/2/3/4/8/11/14/15/17/18/23	84.86%
	X51(T_1b_3)	1/2/3/4/8/11/14/15/17/18/23	86.22%

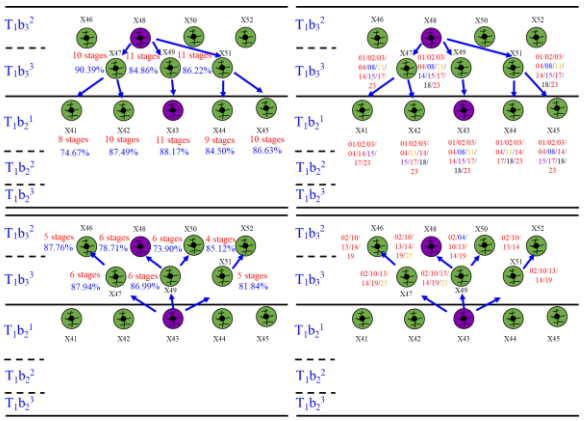

Fig. 8. The skectch map of interlayer interference events

However, the average thickness of the mudstone barrier developed between the formations of T_1b_3 and $T_1b_2^1$ is close to 6m. In the process of fracture stimulation design, stress and rock mechanics evaluation show that it has strong shielding property, and the vertical expansion ability of hydraulic fracture is limited, which is contrary to the actual interference events.

Abnormal Microseismic signals

The attempt of combining the micro seismic surveillance offers an improved understanding of interlayer interference events mentioned in the previous part. Then generous abnormal signals were found that mainly occurred on Pad 2 and Pad 3. Fig.10 shows the map view of micro seismic events for the two pads. And it displays that there are a large number of micro seismic events in the southeast with a strong directivity. Among them, Pad 3 has the most times of this phenomenon. Most of these signals have poor continuity in a wide range (up to about 600m).

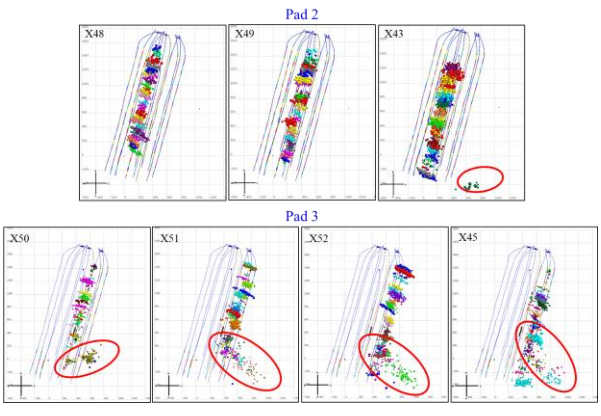

Fig. 9. Abnormal Microseismic Signals

Analysis of Interlayer Interference

Similar phenomena occurred in the Woodford shale and the leading role of faults and fracture warms in hydraulic fracture growth is described in [2]:

- The interaction with local structural features (faults, fracture swarms) had a significant effect on fracture treatment geometry.
- They can completely dominate fracture growth as subsequent stages may continue to grow into the previously intersected fault.

It is a good explanation for the occurrence of abnormal micro seismic signals. To ensure this point, it is necessary to make further analysis with the help of 3D seismic data volume. Fig.11 shows the attributes of 3D seismic data volume in the area of these three Pads. The lateral stability of frequency attribute indicating low-energy or stable sedimentary environment while the large area stability of amplitude attribute reflects the good continuity of overlying and underlying formations.

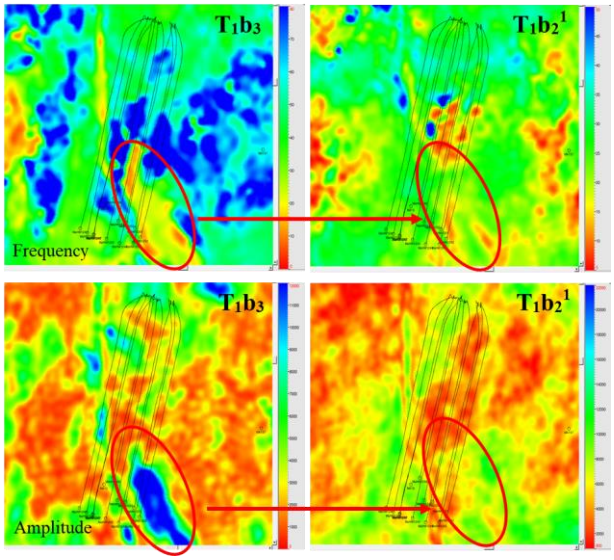

Fig. 10. Attributes of 3D seismic data volume

According to the seismic volume attributes of T_1b_3 and $T_1b_2^1$ formations, the frequency attribute in the southeast of this area rapidly decreases which reflecting the rapid change of lithology. And it is inferred that the rapid lithology change and mudstone interbedding occur in the longitudinal direction. The variation trend of amplitude attribute in this area also reflects the rapid change of lithology of overlying and underlying formations. Through a series of methods, the mechanism of interlayer interference is certain:

- The rapid change of vertical and horizontal lithology results in the occurrence of interbedding of sand and mudstone, which is significant in the southeast.
- Local structural features (faults, fracture swarms) lead the multi-stage repeated stimulations. Besides, the frac-fluid injecting into the weak plane of bedding previously results in the enhancement of the rheological property of mudstone.
- Under the action of high shear stress, mudstone enters into the steady rheology state. The rheological deformation causes the rock fault in the southeast of this area, and abnormal micro-seismic signals happened. Finally, the structural deformation of formations in this area give rise to interlayer interference events.

ACKNOWLEDGMENT

The type of interference (the same layer, cross layer) and the interference layers can be directly determined by the frac-fluid tracer surveillance. Then, correlations of fractured intervals can be calculated through the GRA. And the result is reliable which has strong applicability for analyzing the complex system of seepage flow after fracture stimulation. Compared with the similar phenomena in the Woodford shale, the interlayer interference events concentrated in local faults and fracture swarms may result in the structural deformation of the formation, which may lead to the risk of casing deformation.

REFERENCES

[1] Cherifi, M., Tiab, D., & Escobar, F. H. (2002, January 1). Determination of Fracture Orientation by Multi-Well Interference Testing. Society of Petroleum Engineers. doi:10.2118/77949-MS

[2] Merkle, S., Lehmann, J. and Pyecroft, J. 2013. Field Trial of a Cased Uncemented Multi Fractured Horizontal Well in the Horn River. Society of Petroleum Engineers. Paper URTeC doi: 10.1190/ URTECH2013-138

[3] Fu, Y., Dehghanpour, H., Ezulike, O., Virues, C., & Bearinger, D. (2017, July 24). Investigating Well Interference in a Multi-Well Pad by Combined Flowback and Tracer Analysis. Unconventional Resources Technology Conference. doi:10.15530/URTEC-2017-2697593

[4] Kumar, A., Seth, P., Shrivastava, K., Manchanda, R., & Sharma, M. M. (2018, August 9). Well Interference Diagnosis Through Integrated Analysis of Tracer and Pressure Interference Tests. Unconventional Resources Technology Conference. doi:10.15530/URTEC-2018-2901827

[5] Vulgamore, T. B., Clawson, T. D., Pope, C. D., Wolhart, S. L., Mayerhofer, M. J., Machovoe, S. R., & Waltman, C. K. (2007, January 1). Applying Hydraulic Fracture Diagnostics To Optimize Stimulations in the Woodford Shale. Society of Petroleum Engineers. doi:10.2118/110029-MS

[6] Sardinha, C. M., Petr, C., Lehmann, J., Pyecroft, J. F., & Merkle, S. (2014, September 30). Determining Interwell Connectivity and Reservoir Complexity Through Frac Pressure Hits and Production Interference Analysis. Society of Petroleum Engineers. doi:10.2118/171628-MS

[7] Fu, Y., Dehghanpour, H., Ezulike, O., Virues, C., & Bearinger, D. (2017, July 24). Investigating Well Interference in a Multi-Well Pad by Combined Flowback and Tracer Analysis. Unconventional Resources Technology Conference. doi:10.15530/URTEC-2017-2697593.

[8] J.L. Deng, Introduction to Grey System, The Journal of Grey System (UK) 1 (1) (1989) 1–24.

[9] Y. Kuo, T. Yang, G.W. Huang, The use of grey relational analysis in solving multiple attribute decision-making problems, Computers & Industrial Engineering 55 (1) (2008) 80–93.